



## ARTICLE

# Asialo GM1-positive liver-resident CD8 T cells that express CD44 and LFA-1 are essential for immune clearance of hepatitis B virus

Chi-Chang Sung<sup>1</sup>, Jau-Hau Horng<sup>2</sup>, Shih-Hong Siao<sup>1</sup>, I-Tsu Chyuan<sup>3,4</sup>, Hwei-Fang Tsai<sup>5</sup>, Pei-Jer Chen<sup>6</sup> and Ping-Ning Hsu<sup>1,7</sup>

Persistent hepatitis B virus (HBV) infection results in chronic liver diseases that may progress to chronic hepatitis, liver cirrhosis, and subsequent hepatocellular carcinoma. Previous studies demonstrated that adaptive immunity, in particular CD8 T cells, is critical in HBV elimination. Recent studies have revealed a distinct tissue-localized T cell lineage, tissue-resident memory (TRM) cells, that is crucial for protective immunity in peripheral tissues. In this study, we showed that treatment with an anti-asialo GM1 (ASGM1) antibody (Ab), which depletes NK cells, led to impairment of HBV clearance in a mouse animal model. Unexpectedly, the ability to clear HBV was not significantly impaired in NFIL3 KO mice, which are deficient in NK cells, implying that other non-NK ASGM1-positive immune cells mediate HBV clearance. We isolated intrahepatic ASGM1-positive cells from NFIL3 KO mice and analyzed the immune phenotype of these cells. Our results demonstrated a distinct population of CD44<sup>+</sup> LFA-1<sup>hi</sup> CD8 T cells that were the major intrahepatic ASGM1-positive immune cells in NFIL3 KO mice. Importantly, transcriptome analysis revealed that these ASGM1-positive CD8 T cells had distinct gene profiles and shared a similar core gene signature with TRM cells. In addition to both transcriptional and phenotypic liver residency characteristics, ASGM1-positive CD8 T cells were able to home to and be retained in the liver after adoptive transfer. Taken together, our study results indicate that these ASGM1-positive liver-resident CD8 T cells are the major effector immune cells mediating anti-HBV immunity.

**Keywords:** asialo GM-1; liver-resident CD8 T cells; HBV clearance

*Cellular & Molecular Immunology* (2021) 18:1772–1782; <https://doi.org/10.1038/s41423-020-0376-0>

## INTRODUCTION

Hepatitis B virus (HBV) is a major global health problem causing chronic liver diseases that may progress to chronic hepatitis, liver cirrhosis, and subsequent hepatocellular carcinoma. Adaptive immunity has long been considered a key effector for eliminating HBV,<sup>1–3</sup> nevertheless, the role of innate immunity during HBV infection remains unknown.<sup>4</sup> To explore the role of innate effectors in the response to HBV, we previously investigated a panel of gene knockout (KO) mice with deficiencies in innate immune sensors or effectors to determine their ability to clear HBV.<sup>1</sup> Instead of interferon (IFN) receptor deficiency, interestingly, tumor necrosis factor (TNF)- $\alpha$  deficiency in KO mice resulted in impaired clearance and prolonged persistence of HBV, suggesting that TNF- $\alpha$  and associated innate pathways are crucial for HBV clearance.<sup>1</sup> Although many immune cells produce TNF- $\alpha$ , the role of a key TNF- $\alpha$  producer, natural killer (NK) cells,<sup>5</sup> needs to be elucidated. NK cells, large granular lymphoid-like cells that are now classified as type I innate lymphoid cells (ILCs), play key roles in both innate and adaptive immunity. NK cells are major innate immune cells and are abundant in the liver. Pivotal in vivo

functions of NK cells were illustrated in mice by ablation with NK cell-depleting antibodies (Abs), particularly anti-asialo GM1 (ASGM1).<sup>6–8</sup> It was demonstrated that anti-ASGM1-treated mice failed to clear HBV, which implied that NK cells can enhance HBV-specific CD8 T response and that CD8 T cells were required for protection.<sup>9</sup>

In addition to innate immune cells, recent studies in viral models have now revealed a distinct tissue-localized T cell lineage, tissue-resident memory (TRM) cells, that resides in peripheral tissues and is crucial for protective immunity in peripheral tissues.<sup>10–14</sup> It is now recognized that peripheral tissues, including the liver, are surveyed by TRM cells that vastly outnumber recirculating memory T cells.<sup>15</sup> As a distinct memory T cell lineage, CD8 tissue-resident memory T cells can be distinguished from other T cell subsets by immune markers, including CD44, CD103, CD69, and CD49a.<sup>11–14,16–18</sup>

In this study, we demonstrated that HBV clearance was abolished in mice treated with anti-ASGM1 antiserum. Unexpectedly, the ability to clear HBV was not impaired in nuclear factor, interleukin (IL)-regulated 3 (NFIL3) KO mice with an NK

<sup>1</sup>Graduate Institute of Immunology, College of Medicine, National Taiwan University, Taipei, China; <sup>2</sup>Graduate Institute of Microbiology, College of Medicine, National Taiwan University, Taipei, China; <sup>3</sup>Department of Internal Medicine, Cathay General Hospital, Taipei, China; <sup>4</sup>School of Medicine, College of Medicine, Fu Jen Catholic University, New Taipei City, China; <sup>5</sup>Department of Internal Medicine, Taipei Medical University Shuang Ho Hospital, Taipei, China; <sup>6</sup>Graduate Institute of Clinical Medicine, College of Medicine, National Taiwan University, Taipei, China and <sup>7</sup>Department of Internal Medicine, National Taiwan University Hospital, Taipei, China  
Correspondence: Ping-Ning Hsu (phsu8635@ntu.edu.tw)

Received: 14 September 2019 Accepted: 2 February 2020

Published online: 28 February 2020

cell deficiency. Moreover, the ability to clear HBV was totally abolished when NFIL3 KO mice were treated with anti-ASGM1 antiserum, indicating that other non-NK ASGM1-positive immune cells mediate HBV clearance. We further demonstrated a distinct population of CD44<sup>+</sup> LFA-1<sup>hi</sup> CD8 T cells that were the major intrahepatic ASGM1-positive immune cells and showed liver-resident properties. Our results indicate that ASGM1-positive liver-resident CD8 T cells that express CD44 and LFA-1 are the major effector immune cells mediating anti-HBV immunity.

## MATERIALS AND METHODS

### Animals

All mice used in this study were from a BALB/c or C57BL/6 (B6) background and were 6–8 weeks of age. BALB/c and B6 WT mice were purchased from the National Laboratory Animal Center (Taipei, Taiwan). NFIL3 KO cells were provided by Dr. Tak Mak (The Campbell Family Institute for Breast Cancer Research, Toronto, Canada). All mice were bred and kept in a specific pathogen-free (SPF) facility at the College of Medicine, National Taiwan University (NTU). All experiments and the use of the animals were reviewed and approved by the Institutional Animal Care and Use Committee (IACUC) of the NTU Medical Center.

### Hydrodynamics-based HBV transfection model

Mice (male, 6–8 weeks old) were warmed under a pet lamp and anesthetized with ketamine and xylazine. Ten micrograms of plasmid DNA/Dulbecco's phosphate-buffered saline (DPBS) in a volume equivalent to 8% of the mouse body weight was injected via a tail vein over 5 s. Phosphorylated adeno-associated virus (pAAV)/HBV plasmid DNA was purified using an Endotoxin-Free Maxi plasmid kit (MACHEREY-NAGEL, Düren, Germany). Facial vein blood was collected weekly with a lancet. Serum levels of hepatitis B surface antigen (HBsAg) and anti-hepatitis B surface antibody (anti-HBs Ab) were determined using Roche's cobas e 411 Immunoassay Analyzer (Roche Diagnostics, Mannheim, Germany). Serum HBsAg and anti-HBs Ab levels were assayed at the indicated time points to monitor the state of HBV persistence.

### Detection of the HBV antigen, antibody (Ab), and DNA

Serum levels of HBsAg, anti-HBc, and anti-HBs Abs were determined using an AXSYM system kit (Abbott Diagnostika, Wiesbaden, Germany). The cutoff value for determining HBsAg positivity was a signal-to-noise (S/N) ratio of  $\geq 2$  and a signal-to-cutoff (S/CO) ratio of  $\geq 1$ .

In vivo depletion of NK cells by an anti-asialo GM1 (ASGM1) Ab Lyophilized anti-ASGM1 antiserum (Wako Pure Chemicals, Osaka, Japan) was dissolved in distilled water according to the manufacturer's instructions. For NK cell depletion, mice (male, 6–8 weeks old) were given a 20- $\mu$ l intraperitoneal (i.p.) injection of an anti-ASGM1 antiserum solution 1 day before hydrodynamic transfection and then twice per week for 8–10 weeks. The intrahepatic immune cell population was determined by the immune phenotype by FACS scanning, and NK cell depletion was confirmed by flow cytometry.

### Isolation of intrahepatic lymphocytes (IHLs)

Mice were anesthetized by intravenous administration of 10  $\mu$ l of premixed Zoletil/rompun (Virbac Laboratories, Carros, France), and then the livers of mice were perfused with 10 ml of DPBS. Cells were suspended in Hank's balanced salt solution (HBSS) buffer by mincing the perfused liver with a pestle and passing it through a 70- $\mu$ m strainer (BD Biosciences, San Jose, CA). Hepatocytes and large cell clumps were removed twice by centrifugation at 50  $\times$  g for 5 min. The supernatant containing

intrahepatic leukocytes (IHLs) was pelleted by centrifugation at 300  $\times$  g and 4  $^{\circ}$ C for 10 min. Cells were resuspended in 40%/70% Percoll (GE Healthcare Life Sciences, Chicago, IL) for gradient centrifugation at 1200  $\times$  g for 20 min. Interface cells were washed once with HBSS.

### Analysis of IHLs and splenocytes

Single-cell suspensions were first stained with FC receptor blocker (BD Biosciences, San Jose, CA) for 10 min on ice and then subjected to surface marker-specific Ab staining for 60 min. Cells were labeled with a polyclonal Ab specific for ASGM1 and monoclonal Abs specific for CD3 (17A2), CD8 $\alpha$  (53-6.7), CD25 (pc61.5), CD44 (IM7), CD62L (MEL-14), CD69 (H1.2F3), CD103 (M290), CD107a (1D4B), CD127 (SB/199), CD137 (17B5), CX3CR1 (SA011F11), ICOS (7E.17G9), KLRG1 (2F1), LFA-1 (H155-78), NK1.1 (PK126), PD-1 (29F-1A12), and RANKL (IK22/5) from BioLegend (San Diego, CA). Dead cells were excluded by propidium iodide staining. After being washed once, cells were resuspended in FACS buffer (2% fetal bovine serum (FBS) in phosphate-buffered saline (PBS)) and analyzed by flow cytometry (Canto II, BD Biosciences), or isolated IHLs were further singly stained with an anti-ASGM1, anti-CD44, or anti-LFA-1 Ab for 60 min and then subjected to FACS. Cells were sorted on a FACS Aria IIIu (BD Biosciences, San Jose, CA).

### Immunohistochemistry (IHC)

Perfused livers were fixed in 10% formalin and embedded in paraffin. Intrahepatic HbcAg was detected by IHC staining with rabbit anti-HBc and an Envision System, horseradish peroxidase (DAB) (Dako, Glostrup, Denmark). Hematoxylin was used to stain liver section nuclei.

### Adoptive transfer

For adoptive transfer experiments, recent studies indicated that in vivo blockade of the P2X7 receptor is required to improve the survival of TRM cells.<sup>19,20</sup> To avoid apoptosis of adoptively transferred CD8 T cells, C57BL/6 mice were intravenously administered 1  $\mu$ g of the P2x7 inhibitor KN-62 (Cambridge UK) per mouse. Thirty minutes later, intrahepatic leukocytes were harvested and stained. CFSE-labeled CD8 T cells or sorted ASGM1-positive/negative CD8 T cells from livers of congenic mice (CD45.1/CD45.2) were adoptively transferred intravenously into C57BL/6 mice (CD45.2). A FACSAria cell sorter (BD Biosciences, San Jose, CA) was used to purify ASGM1<sup>+</sup> and ASGM1<sup>-</sup> CD8 T cells. The purity of sorted cells was more than 90%, as verified by flow cytometry. C57BL/6 mice received intravenously  $1 \times 10^5$  donor cells.

### Gene expression profile analysis of ASGM1<sup>+</sup> and ASGM1<sup>-</sup> CD8 T cells

ASGM1<sup>+</sup> and ASGM1<sup>-</sup> CD8 T cells ( $3 \times 10^4$ ) from the livers of naive NFIL3 KO mice were sorted on a FACSAria III (BD Biosciences, San Jose, CA). For each sample, we extracted total RNA using TRIzol (Invitrogen, Waltham, MA). After amplification and conversion to cDNA, samples were hybridized to an Affymetrix transcriptome array (Mouse Clariom D) (Affymetrix Inc., Santa Clara, CA) at the NCFPB High-throughput Genome Analysis Core Facility. Image analysis was performed using Affymetrix Transcriptome Analysis Suite (TAS) (Affymetrix Inc., Santa Clara, CA) (GEO series accession number: GSE137767).

### Quantitative PCR analysis of ASGM1<sup>+</sup> and ASGM1<sup>-</sup> CD8 T cells

For quantitative PCR, total RNA was isolated from the indicated cells using TRIzol (Invitrogen, Waltham, MA), and cDNA was synthesized with iScript (Bio-Rad, Hercules, CA) according to the manual. Quantitative amplification was performed with SYBR Premix ExTaq II (TaKaRa, Shiga, Japan) in a Thermo PIKOREAL 96 system (Thermo Fisher Scientific, Vantaa, Finland) with the

following primers: Inpp4b: 5'-CAGTAGCAAGGATGGAGAGGCA-3' (forward), 5'-TTGCTCGGTTCCACCTT CTCC-3' (reverse); Itgae: 5'-GAAGTGGAAACGGAG GGTCTTT-3' (forward), 5'-GTCTGGAACCTCG TAGGTGACCT-3' (reverse); Eomes: 5'-CCACTGGATGAG GCAGGAG ATT-3' (forward), 5'-GTCCTGTGCTACTTCCACGATG-3' (reverse); and Ly6C2: 5'-GCGCCTCTGATGGATTCTGCAT-3' (forward), 5'-TCCTTG ATTGGCACACCAGCAG-3' (reverse) (PURIGO, Taipei, Taiwan).

#### Statistical analyses

Student's *t*-test was used to compare two experimental groups, and a *P*-value of less than 0.05 was defined as statistically significant.

## RESULTS

Anti-ASGM1 treatment significantly impaired HBV clearance in a mouse animal model

To study the role of NK cells in HBV clearance, an anti-ASGM1 Ab was i.p. injected into BALB/c or C57BL/6 mice to deplete NK cells. The percentages of NK cells in the liver were markedly decreased in mice treated with the anti-ASGM1 Ab (Fig. 1a, e). Per the results shown in Fig. 1, after a hydrodynamic injection (HDI) of replication-competent HBV DNA, anti-ASGM1-treated mice remained HBsAg seropositive until the endpoint, with a significantly higher serum HBsAg titer than mice treated with an isotype control (Fig. 1b, f). The development of anti-HB Abs in serum was delayed in mice treated with the anti-ASGM1 Ab compared to that in the control group mice (Fig. 1d, h). Moreover, IHC analysis revealed that staining for HBcAg remained detectable in the livers of anti-ASGM1-treated BALB/c and C57BL/6 mice at day 42 post-transfection. In contrast, staining signal for HBcAg was much lower in control mice (Fig. 1c, g). Taken together, our results indicated that anti-ASGM1 treatment significantly impaired the ability to clear HBV in both BALB/c and C57BL/6 mice, indicating that ASGM1-expressing immune cells mediate the anti-HBV immune response needed to clear the virus.

NK cell-deficient mice, NFIL3 KO mice, maintain immune competence to clear HBV

To further investigate the role of NK cells in HBV clearance, we employed NFIL3 KO mice, which are deficient in NK cells and ILCs,<sup>21,22</sup> in this HBV mouse animal model. As shown in Fig. 2a, the percentages of NK cells were markedly lower in NFIL3 KO mice than in wild-type (WT) C57BL/6 mice. Unexpectedly, after HDI with HBV DNA, the ability to clear HBV in NFIL3 KO mice was comparable to that in WT mice, as determined by serum levels of HBsAg (Fig. 2b). Similarly, there was no significant difference in the production of anti-HB Abs between NFIL3 KO and WT mice (Fig. 2d). In addition, HBcAg expression within liver tissues was almost completely cleared 6 weeks after the HDI in both NFIL3 KO and WT mice (Fig. 2c). Taken together, the results demonstrated that NFIL3 KO mice were functionally competent in HBV clearance, suggesting that NK cells are not the key effector cells for HBV clearance. This result raises the possibility that there are other non-NK, ASGM1-positive immune cells that may mediate the anti-HBV immune response to clear the virus.

Intrahepatic ASGM1-positive but non-NK immune cells mediate HBV clearance

To confirm the possibility that there are other non-NK, ASGM1-positive immune cells that may mediate HBV clearance, we further treated NFIL3 KO mice with anti-ASGM1 Abs to evaluate the impact on HBV clearance. The results in Fig. 3a demonstrate that the HBsAg level was persistently elevated in anti-ASGM1-treated NFIL3 KO mice after the HDI. None of the

anti-ASGM1-treated mice were found to produce anti-HB Abs in the serum; in contrast, significantly increased anti-HB Ab levels developed after the HDI in control mice (Fig. 3b). In addition, HBcAg in the liver was persistently detected by IHC staining in anti-ASGM1-treated mice for up to 6 weeks after the HDI (Fig. 3c). These results indicate that there are other non-NK, ASGM1-positive immune cells that could be depleted by anti-ASGM1 antiserum and mediated HBV clearance in NFIL3 KO mice.

ASGM1-positive CD8 T cells are the predominant intrahepatic immune cells in NFIL3 KO mice

To further search for the non-NK, ASGM1-positive immune cells that mediate the anti-HBV immune response, we sorted intrahepatic ASGM1-positive cells from WT and NFIL3 KO mice and analyzed their immune phenotype. As shown in Fig. 4, the percentage of NK1.1<sup>+</sup>CD3<sup>-</sup> cells was significantly higher in IHLs from WT mice than in IHLs from NFIL3 KO mice, consistent with the notions that conventional NK cells express high levels of ASGM1 and that they are the predominant cell type among ASGM1-positive cells. In contrast, in NFIL3 KO mice, the major immune cell type in sorted ASGM1-positive IHLs was NK1.1<sup>-</sup>CD3<sup>+</sup> T cells (Fig. 4a). Furthermore, the percentage of CD8<sup>+</sup> T cells was significantly higher than that of CD4<sup>+</sup> T cells in sorted ASGM1<sup>+</sup> cells (Fig. 4c, d). In addition, anti-ASGM1 treatment depleted intrahepatic HBcAg-specific CD8 T cells in NFIL3 KO mice (Supplementary Fig. S1). All of these results indicate that these ASGM1-positive CD8 T cells are the major effector immune cells mediating HBV clearance in NFIL3 KO mice.

The major intrahepatic ASGM1-positive immune cells in NFIL3 KO mice are CD44<sup>+</sup> LFA-1<sup>+</sup> CD8 T cells

CD8 T cells are considered one of the key effector immune cells in HBV clearance. CD8 T cell-depleted chimpanzees and CD8 KO mice were shown to lose the ability to clear HBV.<sup>2,23</sup> Restoration of T cell function by PD-1 blockade supported the importance of regulation of CD8 T cell effector function in animal models of HBV infection.<sup>24</sup> This finding raises the possibility that ASGM1-positive CD8 T cells belong to a distinct population of effector CD8 T cells that mediate the immune response for HBV clearance within the liver. Therefore, we evaluated a panel of activation markers and immunophenotypes of intrahepatic CD8 T cells from NFIL3 KO mice (Figs. 5 and S2). The results in Figs. 5 and S2 demonstrate that among intrahepatic ASGM1-positive CD8 T cells, most expressed CD44, CD69, and LFA-1. By comparing CD44, LFA-1, and ASGM1 expression patterns in intrahepatic CD8 T cells from NFIL3 KO mice, the overlapping intersection occupied almost all of the LFA-1<sup>hi</sup> population and the majority of the ASGM1 set (Fig. 5a, b), implying that the anti-ASGM1 Ab could deplete almost all of the intrahepatic LFA-1<sup>hi</sup>CD44<sup>+</sup> CD8 T cells. To further confirm that the anti-ASGM1 Ab can deplete almost all CD44<sup>+</sup> LFA-1<sup>hi</sup> CD8 T cells, we injected mice with the anti-ASGM1 Ab, and the results in Fig. 5c demonstrated that after treating mice with the anti-ASGM1 Ab, most of the CD44<sup>+</sup> LFA-1<sup>hi</sup>, as well as CD44<sup>+</sup> CD69<sup>+</sup> CX3CR1<sup>-</sup> CD8 T cells in WT or NFIL3 KO mice, were depleted. Taken together, our results indicate that distinct CD44<sup>+</sup> LFA-1<sup>hi</sup> CD8 T cells, a population of liver-resident CD8 T cells, were the major intrahepatic ASGM1-positive immune cells. These CD44<sup>+</sup> LFA-1<sup>hi</sup> CD8 T cells could be depleted by an anti-ASGM1 Ab in vivo. Moreover, the intrahepatic ASGM1<sup>+</sup> LFA-1<sup>hi</sup> CD8 T cell population significantly increased after mice underwent HDI with HBV DNA (Fig. S3). The intrahepatic ASGM1<sup>+</sup> CD8 T cells expressed higher levels of PD-1 and CD69 in HBV-transfected mice than in naive mice (Fig. S4). Our results demonstrated that ASGM1<sup>+</sup> CD44<sup>+</sup> LFA-1<sup>hi</sup> CD8 T cells were phenotypically liver resident and were present in both naive and HBV-transfected mice.



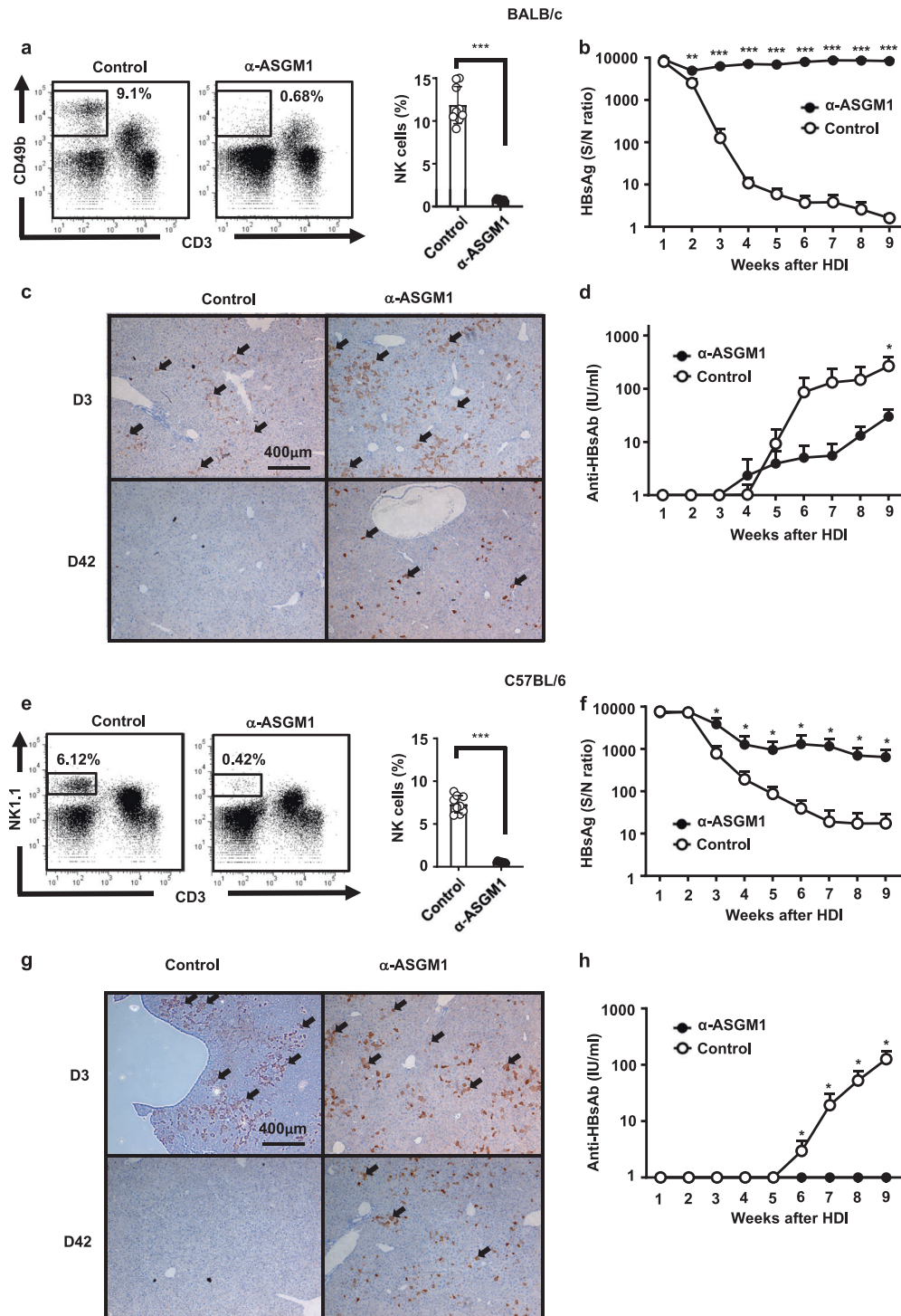


**Fig. 1** Anti-asialo GM1 (ASGM1) antibody treatment significantly impaired hepatitis B virus (HBV) clearance. **a** BALB/c mice at 6–7 weeks old were treated with anti-ASGM1 antiserum or an isotype control. Intrahepatic leukocytes were isolated, and the natural killer (NK) cell frequency was analyzed by flow cytometry. A representative flow cytometric analysis of NK cells (left) and their frequency (right panel) is shown. **b–d** BALB/c mice ( $n = 10$ ) underwent hydrodynamic injection (HDI) with adeno-associated virus (pAAV)/HBV1.2 plasmids in the presence or absence of anti-ASGM1 treatment. Anti-ASGM1 treatment was performed twice per week over the detection period. Serum titers of HBsAg (**b**) and anti-HBs Ab (**d**) at the indicated times were determined by ELISA. **c** IHC staining for HBcAg expression in the livers (arrow) of anti-ASGM1-treated BALB/c mice compared to that in the livers of control mice on days 3 and 42 after pAAV/HBV1.2 injection. Data are shown as the mean  $\pm$  SEM. \* $p < 0.05$ , \*\* $p < 0.01$ , \*\*\* $p < 0.001$  between selected relevant comparisons by Student's *t*-test. **e** C57BL/6 mice ( $n = 10$ ) at 6–7 weeks old were treated with anti-ASGM1 antiserum or an isotype control. Intrahepatic leukocytes were isolated, and the natural killer (NK) cell frequency was analyzed by flow cytometry. A representative flow cytometric analysis of NK cells (left) and their frequency (right panel) is shown. **f–h** C57BL/6 mice ( $n = 10$ ) were HDI with pAAV/HBV1.2 plasmids in the presence or absence of anti-ASGM1 treatment. Anti-ASGM1 or isotype antibody treatment was performed twice per week over the detection period. Serum titers of HBsAg (**f**) and anti-HBsAb (**h**) were measured at the indicated times. **g** IHC staining of HBcAg expression in the liver (arrow) on days 3 and 42 after pAAV/HBV1.2 injection. Data are shown as the mean  $\pm$  SEM. \* $p < 0.05$ , \*\* $p < 0.01$ , \*\*\* $p < 0.001$  between selected relevant comparisons by Student's *t*-test

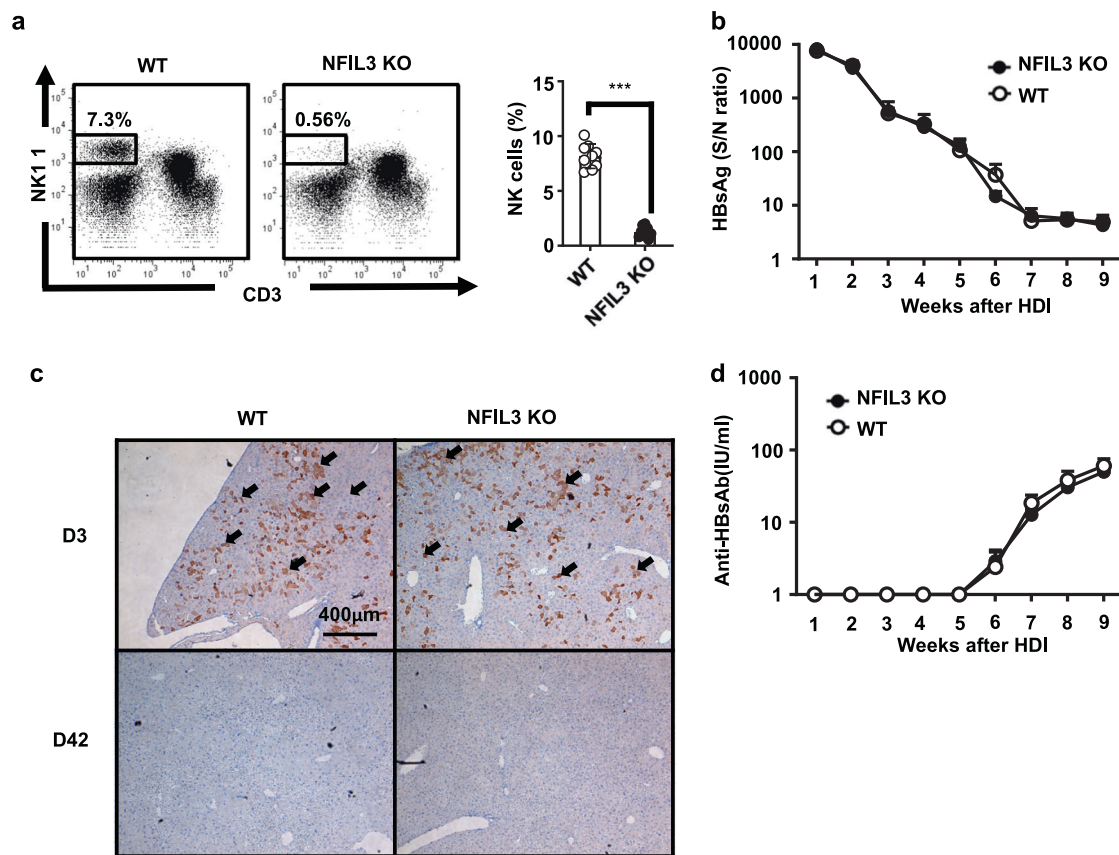


**Fig. 2** NK cell-deficient mice, NFIL3 KO mice, maintain immune competence to clear HBV. **a** Intrahepatic leukocytes of C57BL/6 and NFIL3 KO mice were isolated, and the NK cell frequency was analyzed by flow cytometry. A representative flow cytometric analysis of NK cells (left) and their frequency (right panel) is shown. **b–d** C57BL/6 ( $n = 10$ ) and NFIL3 KO ( $n = 8$ ) mice at 6–7 weeks old underwent hydrodynamic injection (HDI) with adeno-associated virus (pAAV)/HBV1.2 plasmids. Serum titers of HBsAg (**b**) and anti-HBs Ab (**d**) at the indicated times after HDI were determined by ELISA. (**c**) IHC staining for HBcAg expression in the livers of anti-ASGM1-treated and control mice on days 3 and 42 after HDI. Data are shown as the mean  $\pm$  SEM. Statistics were calculated by Student's *t*-test

Intrahepatic ASGM1-positive CD8 T cells have distinct transcriptional profiles and show similarity to the core gene signature of TRM cells

To determine whether the intrahepatic ASGM1-positive CD8 T cells belong to a distinct subset of tissue-resident CD8 T cells, we next examined whether the ASGM1<sup>+</sup> and ASGM1<sup>-</sup> CD8 T cells differ not only in the phenotypic marker but also in their transcriptional signature. Both cell populations were sorted for gene expression microarray analysis. The results from Fig. 6a demonstrated a fold change of two or greater among the 1,129 expressed genes, indicating that ASGM1<sup>+</sup> CD8 T cells were distinct from ASGM1<sup>-</sup> CD8 T cells at the transcriptional level. The differentially expressed genes included those encoding chemokine signaling pathway, T cell receptor signaling pathway, integrin-mediated cell adhesion, focal adhesion, and XPodNet protein-protein interaction factors (Fig. 6b). This result raised the possibility that ASGM1<sup>+</sup> CD8 T cells have unique adhesive properties to mediate retention in the liver. Moreover, many expressed genes in intrahepatic ASGM1<sup>+</sup> CD8 T cells showed similarity to the core gene signature of TRM cells<sup>11,25</sup> (Fig. 6c), and some of these genes were also confirmed by qPCR (Fig. 6d). All these results suggest that these ASGM1<sup>+</sup> CD8 T cells are liver-resident memory T cells.

Intrahepatic ASGM1<sup>+</sup> CD8 T cells homed to and were retained in the liver after adoptive transfer

Recent evidence indicates that large numbers of resident CD8 T cells are harbored within the liver for protection against

pathogen challenges.<sup>26</sup> Nevertheless, whether liver-resident CD8 T cells contribute to the major role of CD8 T cells in host protection against HBV is still unclear. Our results indicate that the major intrahepatic ASGM1-positive immune cells in NFIL3 KO mice highly coexpressed LFA-1, which was recently reported as a phenotypic marker of liver-resident T cells.<sup>14,27</sup> To address the liver-resident role of intrahepatic ASGM1<sup>+</sup> CD8 T cells, we further examined the liver trafficking and retention abilities of these ASGM1<sup>+</sup> CD8 T cells. As shown in Fig. 7a, LFA-1 was highly expressed only in intrahepatic ASGM1<sup>+</sup> CD8 T cells but not in splenic ASGM1<sup>+</sup> CD8 T cells. Moreover, when CFSE-labeled intrahepatic and splenic ASGM1<sup>+</sup> CD8 T cells were sorted and adoptively transferred into recipient mice, only the intrahepatic ASGM1<sup>+</sup> CD8 T cells but not ASGM1<sup>-</sup> or splenic CD8 T cells homed to the livers of recipients after adoptive transfer (Fig. 7b). Similar results were obtained when the intrahepatic ASGM1-positive CD8 T cells from congenic mice (CD45.1/CD45.2) were adoptively transferred intravenously into C57BL/6 mice (CD45.2), and these liver-homing donor cells were able to persist for more than two weeks (Fig. 7c). In addition, after the treatment of mice with the anti-ASGM1 Ab, the liver-resident CD69<sup>+</sup> LFA-1<sup>hi</sup> CD8 T cells were markedly depleted (Fig. 7d). Taken together, our results indicate that intrahepatic ASGM1-positive CD8 T cells, which express CD44 and LFA-1, are a distinct T cell population and that these cells not only phenotypically but also functionally showed liver residency.

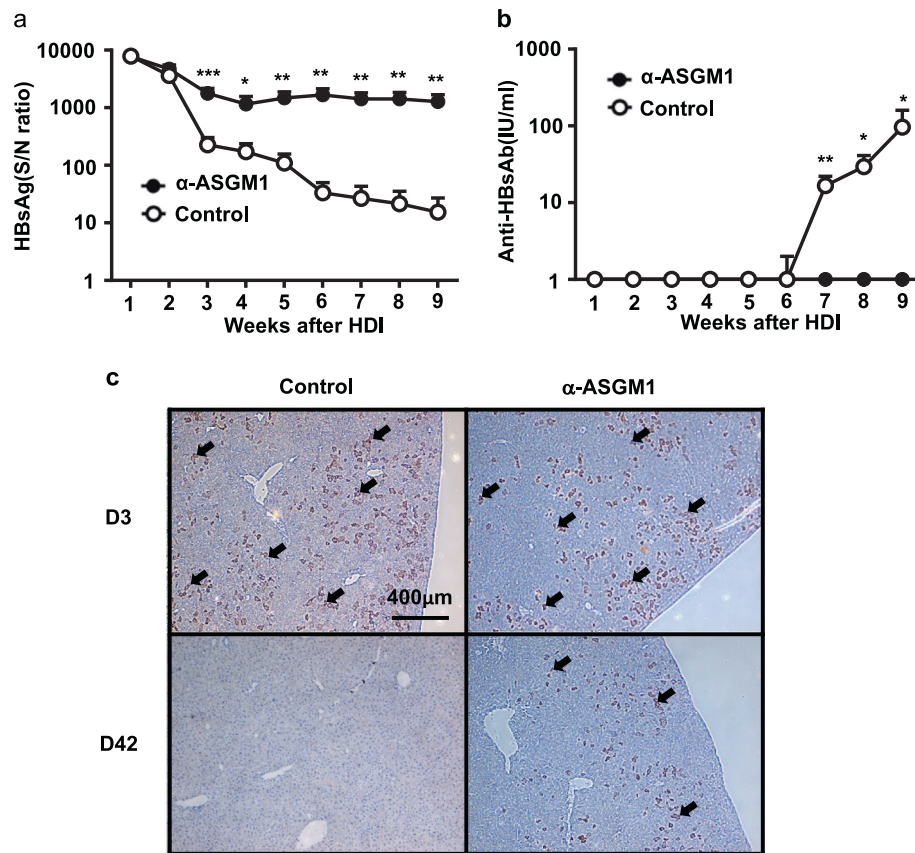


**Fig. 3** Anti-ASGM1 treatment abolished the ability to clear HBV in NFIL3 knockout (KO) mice. **a**, **b** NFIL3 KO mice underwent hydrodynamic injection (HDI) with adeno-associated virus (AAV)/HBV1.2 plasmids in the presence or absence of anti-ASGM1 treatment ( $n = 10$  for each group). Anti-ASGM1 treatment was performed twice per week over the detection period. Serum titers of HBsAg (**a**) and anti-HBs Ab (**b**) at the indicated times were determined by ELISA. **(c)** IHC staining for detection of HBCAg expression in liver tissues (arrow) in NFIL3 KO mice with or without anti-ASGM1 treatment on days 3 and 42 after HDI. Data are shown as the mean  $\pm$  SEM. \* $p < 0.05$ , \*\* $p < 0.01$ , \*\*\* $p < 0.001$  between selected relevant comparisons by Student's  $t$ -test

## DISCUSSION

In this study, we demonstrated that instead of NK cells, an anti-ASGM1 Ab depletes a CD44- and LFA-1-positive liver-resident CD8 T cell population and impairs the immune response to HBV clearance. Our results indicate that ASGM1-positive CD8 T cells that express CD44 and LFA-1 are the major effector immune cells mediating anti-HBV immunity. NK cells are major innate immune cells and are abundant in the liver. However, due to limitations of experimental systems, the actual role of NK cells in anti-HBV immunity is still unclear. In the past decade, researchers have investigated the roles of NK cells using anti-ASGM1 treatment to deplete NK cells in vivo.<sup>6–8</sup> The discrepancy between anti-ASGM1 treatment and NFIL-3 KO mice suggests that there are some differences in immune responses to HBV between anti-ASGM1 Ab-depleted and NK cell-deficient mice. Furthermore, in our study, the ability to clear HBV was abolished when NFIL3 KO mice were further treated with anti-ASGM1 Abs (Fig. 3), implying that there are other non-NK ASGM1-positive immune cells that mediate HBV clearance. Nevertheless, treatment with anti-ASGM1 Abs does not lead to the depletion of tissue-resident NK cells,<sup>28</sup> therefore, the results in this study do not exclude a role for tissue-resident NK cells.

For more than 30 years, anti-ASGM1-mediated NK cell depletion has been demonstrated to be effective in a variety of mouse strains,<sup>6,7</sup> and this approach remains a powerful tool for analyzing NK cell functions in vivo. Nevertheless, the expression of ASGM1 is not strictly confined to NK cells, making depletion also affective against a subpopulation of NKT, CD8 T,

and other hematopoietic cells under certain experimental conditions.<sup>29</sup> Approximately 10% of naive CD8 T cells<sup>30</sup> express ASGM1, but the characteristics of these T cells and the biological roles of these T cells remain undetermined. It was demonstrated that in lymphocytic choriomeningitis virus (LCMV) infection, most virus-specific CD8 T cells express ASGM1 at 8 days post-infection,<sup>31</sup> while whether they are functionally different from ASGM1-negative T cells remains unknown as well. In this study, we further demonstrated that ASGM1-positive CD8 T cells are the predominant intrahepatic immune cells in NFIL3 KO mice and that the majority of these ASGM1-positive immune cells were CD44<sup>+</sup> LFA-1<sup>hi</sup> CD8 T cells, with the phenotype of liver-resident T cells. Herein, we provide the first evidence that instead of NK cells, an anti-ASGM1 Ab depleted a CD44- and LFA-1-positive liver-resident CD8 T cell population and impaired the immune response to HBV clearance. Meanwhile, it has been demonstrated that recently activated CD8 T cells express ASGM1 and can be depleted by anti-ASGM1 treatment.<sup>32</sup> It is still possible that the effects of anti-ASGM1 treatment on HBV clearance are partly due to depletion of effector CD8 T cells. In addition, in this study, depletion of ASGM1+ cells, which prevented viral clearance, led to impaired anti-HBs Ab production. This result suggests that anti-ASGM1 treatment may also deplete effector T cells, which help B cells produce anti-HBs Abs.

It is now recognized that peripheral tissues, including the liver, are surveyed by TRM cells that vastly outnumber recirculating memory T cells.<sup>15</sup> Although the liver was previously thought to be



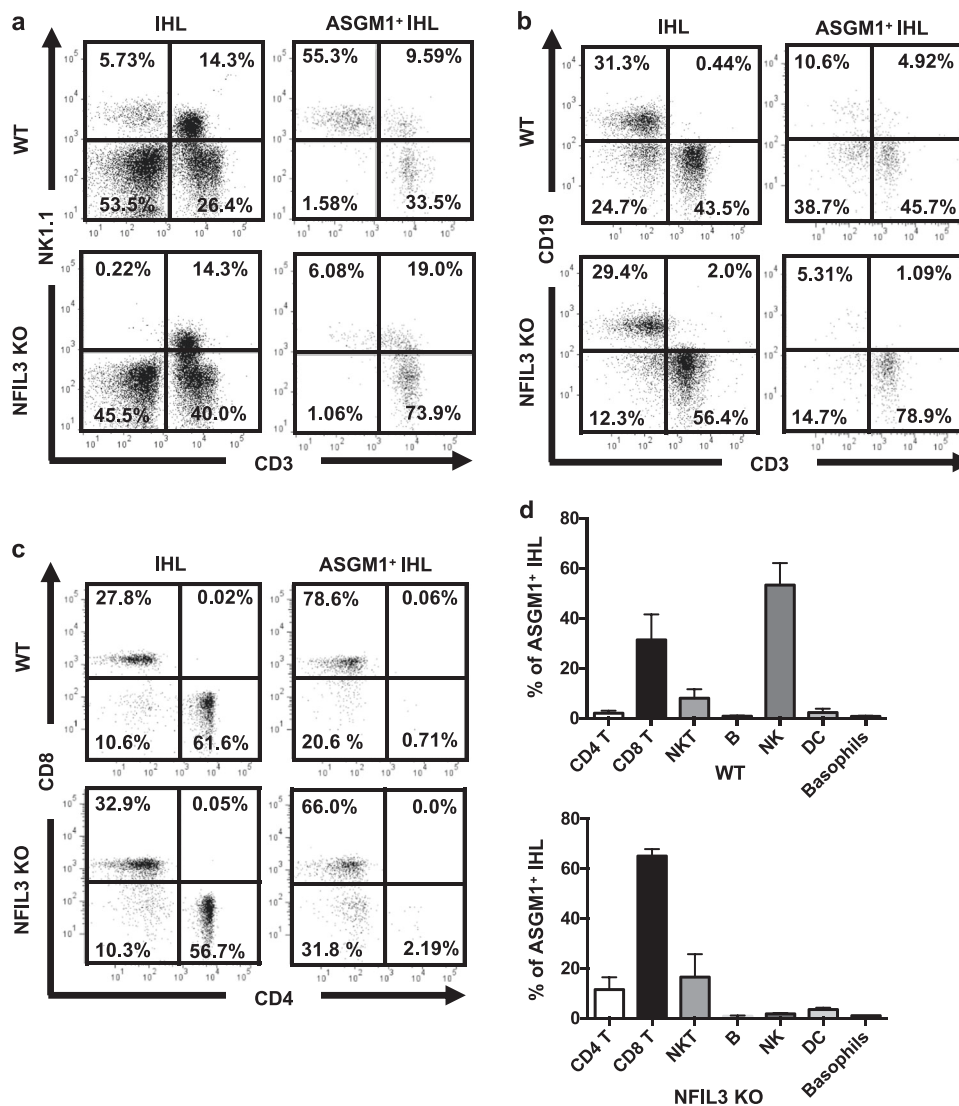


**Fig. 4** ASGM1-positive CD8 T cells are the predominant intrahepatic immune cells in NFIL3 KO mice. Intrahepatic leukocytes of naive C57BL/6 and NFIL3 KO mice were isolated and stained with anti-ASGM1 antibodies. ASGM1<sup>+</sup> cells were further sorted from intrahepatic leukocytes (IHLs) using a FACS Aria IIIu (BD Biosciences, San Jose, CA). The immune phenotypes of NK cells (a), B and T cells (b), and CD4 and CD8 T cells (c) in these ASGM1-positive IHLs were analyzed by flow cytometry. d Quantification of the percentages of the indicated cells in ASGM1-positive IHLs from NFIL3 KO mice is shown

an immune-tolerant organ, recent evidence indicates that distinct tissue-resident memory CD8 T cells are harbored within the liver for protection against pathogens.<sup>26</sup> A population of CD8 TRM cells residing in the human liver, which express tissue retention signals, is expanded upon HBV infection.<sup>33</sup> In addition, it has been shown that liver-resident memory CD8 T cells are present in the murine liver during malaria infection.<sup>11,14,34</sup> These liver-resident memory T cells share a common gene expression signature with epithelium-resident memory T cells.<sup>11,25</sup> However, there are some distinct features compared to epithelium-resident T cells; in particular, liver-resident memory T cells do not express high levels of CD103,<sup>11,25</sup> a key integrin for T cell residence in epithelial tissues.<sup>35</sup> Instead, liver-resident memory CD8 T cells patrolling the liver are dependent upon LFA-1-intracellular adhesion molecule-1 (ICAM-1) interactions. LFA-1-deficient CD8 T cells fail to form substantial liver-resident memory populations, and adhesion through LFA-1 allows liver-resident memory CD8 T cells to patrol and remain in hepatic sinusoids.<sup>14</sup> Our current study results demonstrated a distinct CD44<sup>+</sup> LFA-1<sup>hi</sup> CD8 T cell population of

liver-resident CD8 T cells, which were the major intrahepatic ASGM1-positive immune cells. Asialo-GM1 may not be involved in adhesion for all TRM cells, but most liver-enriched immune cells seem to express ASGM1. Meanwhile, NK cells, which are known to express high levels of ASGM1, are especially enriched in the liver, implying that the expression of ASGM1 may have a role in liver residency. On the other hand, it has been shown that Tcm CD8 T cells can express ASGM1.<sup>30</sup> Therefore, it is possible that the ASGM1-positive CD8 T cell population in our study is a mixture of circulatory and liver-resident cells. Further exploration for more liver-resident markers to identify pure liver-resident T cells is still needed. In this study, we demonstrated that only ASGM1-positive but not ASGM1-negative IHLs play a critical role in HBV clearance. Moreover, these CD44<sup>+</sup> LFA-1<sup>hi</sup> CD8 T cells could be depleted by anti-ASGM-1 Abs in vivo. Taken together, our study results indicate that ASGM1-positive liver-resident CD8 T cells that express CD44 and LFA-1 are the major effector immune cells mediating anti-HBV immunity. Our results also implicate ASGM-1 as a liver-resident marker for immune cells.

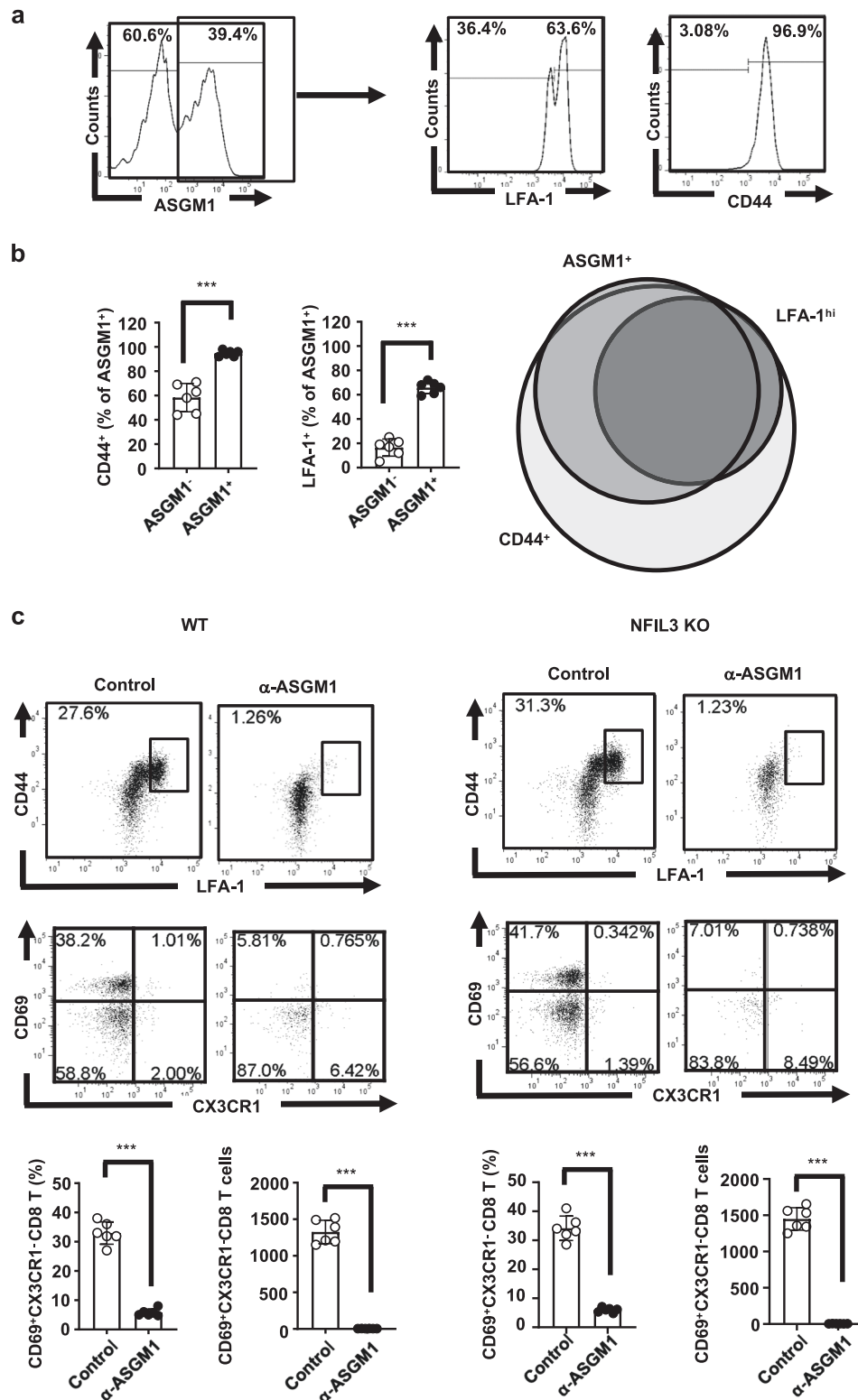


**Fig. 5** The major intrahepatic ASGM1-positive immune cells in NFIL3 KO mice were CD44<sup>+</sup> LFA-1<sup>+</sup> CD8 T cells. **a** Intrahepatic leukocytes (IHLs) from naive NFIL3 KO mice were isolated. Among CD8 T cells, the expression of ASGM1, CD44, and LFA-1 was examined. **b** Quantification of CD44<sup>+</sup> and LFA-1<sup>+</sup> cells among ASGM1<sup>+</sup> CD8 T cells from (a) is shown. The right figure presents a Venn diagram showing the overlap among ASGM1-, CD44-, and LFA-1-positive cells from each group. **c** C57BL/6 (*n* = 6) and NFIL3 KO mice (*n* = 6) were injected with 20 μl of an anti-ASGM1 Ab. One day later, IHLs were harvested, stained, and analyzed by flow cytometry. A representative flow cytometric analysis of CD44<sup>+</sup> LFA<sup>hi</sup> and CD44<sup>+</sup> CD69<sup>+</sup> CX3CR1<sup>-</sup> CD8 T cells in both wild-type and NFIL3 KO mice and their frequency, as well as cell numbers, is shown. Most of the CD44<sup>+</sup> LFA<sup>hi</sup>, as well as CD44<sup>+</sup> CD69<sup>+</sup> CX3CR1<sup>-</sup> CD8 T cells in both wild-type and NFIL3 KO mice, were depleted after treatment with the anti-ASGM1 Ab. \**p* < 0.05, \*\**p* < 0.01, \*\*\**p* < 0.001 between selected relevant comparisons by Student's *t*-test



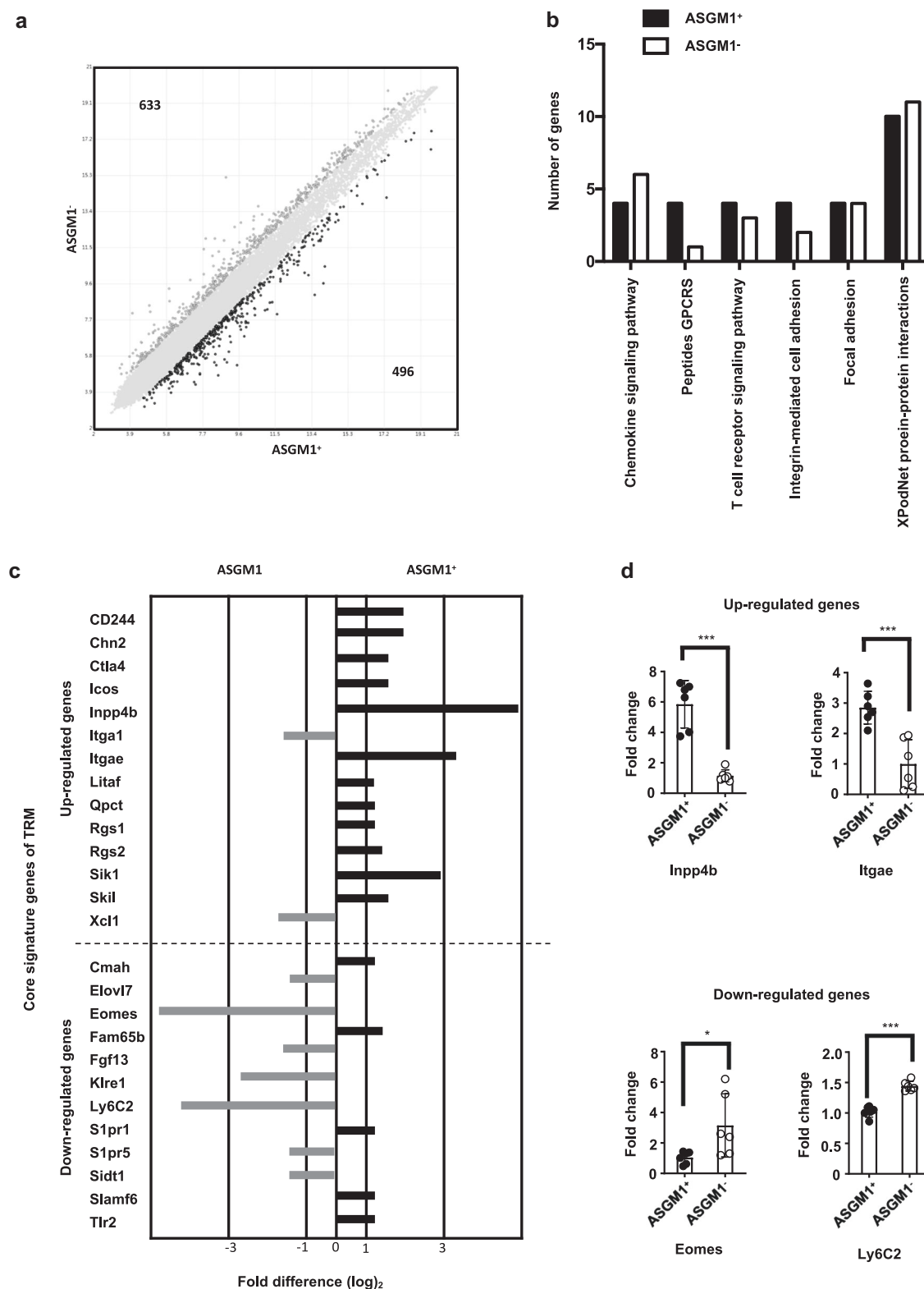


**Fig. 6** Intrahepatic ASGM1<sup>+</sup> CD8 T cells have a distinct transcriptional profile from that of ASGM1<sup>-</sup> CD8 T cells. **a** Comparative transcriptome analysis between ASGM1<sup>+</sup> and ASGM1<sup>-</sup> liver CD8 T cells was performed by Affymetrix GeneChip Mouse arrays (Mouse Clariom D). Genes that were expressed greater than or equal to 2-fold higher or lower than in ASGM1<sup>-</sup> liver CD8 T cells are highlighted in black. The number of genes upregulated or downregulated for each comparison is indicated. **b** Distribution by functional category of upregulated genes in hepatic ASGM1<sup>+</sup> and ASGM1<sup>-</sup> CD8 T cell subsets. Genes with greater than or equal to 2-fold differences were included. **c** Fold change expression of tissue-resident memory T cell core signature genes<sup>35</sup> in ASGM1<sup>+</sup> cells relative to that in ASGM1<sup>-</sup> CD8 T cells. **d** Quantitative PCR analysis of representative liver-resident memory T cell core signature genes in intrahepatic ASGM1<sup>+</sup> CD8 T cells. \**p* < 0.05, \*\**p* < 0.01, \*\*\**p* < 0.001 between selected relevant comparisons by Student's *t*-test

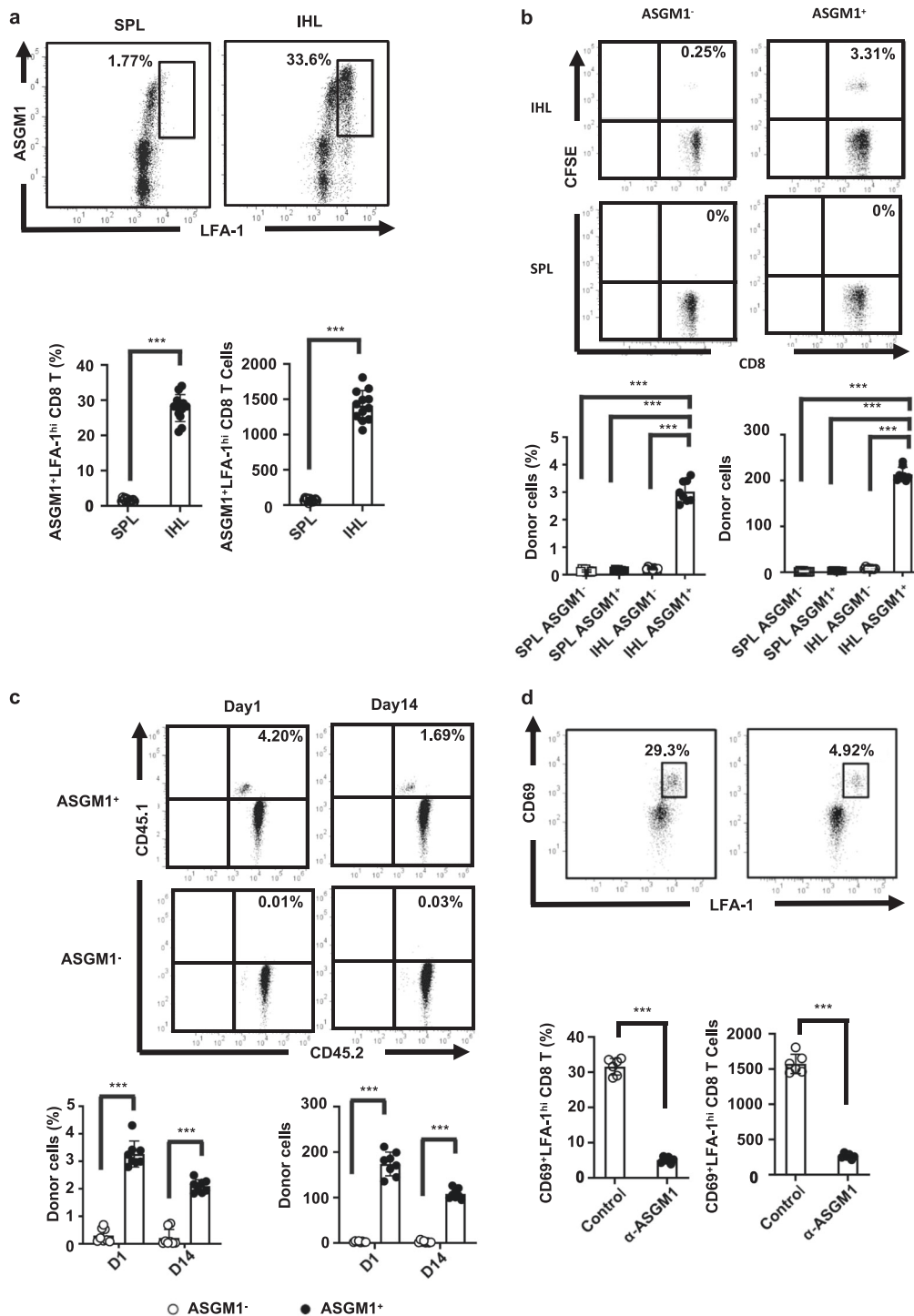


**Fig. 7** The intrahepatic ASGM1-positive CD8 T cells showed liver-resident properties. **a** Intrahepatic and splenic CD8 T cells from NFIL3 KO mice were purified and stained for flow cytometry analysis. A representative flow cytometric analysis of the expression of LFA-1 versus ASGM1 in CD8 T cells and their frequency (lower left panel), as well as cell numbers (lower right panel), is shown. **b** ASGM1-positive or ASGM1-negative CD8 T cells from livers or spleens were stained with CFSE, and then the CFSE-labeled CD8 T cells were sorted via a FACSria cell sorter (BD Biosciences, San Jose, CA). The sorted cell populations were adoptively transferred intravenously into C57BL/6 mice ( $n = 8$ ). One day later, intrahepatic leukocytes were harvested, stained, and analyzed by flow cytometry. A representative flow cytometric analysis of donor CFSE-positive CD8 T cells and their frequency (lower left panel), as well as cell numbers (lower right panel), is shown. **c** Sorted ASGM1-positive or ASGM1-negative CD8 T cells from livers of congenic mice (CD45.1/CD45.2) were adoptively transferred intravenously into C57BL/6 mice (CD45.2) ( $n = 8$ ). One day and 2 weeks after transfer, intrahepatic leukocytes were harvested, stained, and analyzed by flow cytometry. A representative flow cytometric analysis of donor CD45.1-positive CD8 T cells and their frequency (lower left panel), as well as cell numbers (lower right panel), is shown. **d** NFIL3 KO mice ( $n = 6$ ) were injected with 20  $\mu$ l of an anti-ASGM1 Ab. One day later, intrahepatic IHLs were harvested and stained. Among CD8<sup>+</sup> T cells, the expression of LFA-1 versus CD69 was examined. A representative flow cytometric analysis of LFA-1<sup>hi</sup>- and CD69-positive CD8 T cells and their frequency (lower left panel) as well as cell numbers (lower right panel) is shown. \* $p < 0.05$ , \*\* $p < 0.01$ , \*\*\* $p < 0.001$  between selected relevant comparisons by Student's *t*-test

## ACKNOWLEDGEMENTS

This work was supported by grants from the Ministry of Science and Technology (MOST 105-2320-B-038-065, MOST 106-2320-B-038-0193, MOST 107-2321-B-002-003, and MOST 108-2320-B-002-036-MY3).

## ADDITIONAL INFORMATION

The online version of this article (<https://doi.org/10.1038/s41423-020-0376-0>) contains supplementary material.

**Competing interests:** The authors declare no competing interests.

## REFERENCES

1. Tzeng, H. T. et al. Tumor necrosis factor- $\alpha$  induced by hepatitis B virus core mediating the immune response for hepatitis B viral clearance in mice model. *PLoS ONE* **9**, e103008 (2014).
2. Yang, P. L. et al. Immune effectors required for hepatitis B virus clearance. *Proc. Natl Acad. Sci. USA* **107**, 798–802 (2010).
3. Yeo, W. et al. Hepatitis B virus reactivation in lymphoma patients with prior resolved hepatitis B undergoing anticancer therapy with or without rituximab. *J. Clin. Oncol.* **27**, 605–611 (2009).
4. Wieland, S., Thimme, R., Purcell, R. H. & Chisari, F. V. Genomic analysis of the host response to hepatitis B virus infection. *Proc. Natl Acad. Sci. USA* **101**, 6669–6674 (2004).
5. Kashii, Y., Giorda, R., Herberman, R. B., Whiteside, T. L. & Vujanovic, N. L. Constitutive expression and role of the TNF family ligands in apoptotic killing of tumor cells by human NK cells. *J. Immunol.* **163**, 5358–5366 (1999).
6. Kasai, M., Iwamori, M., Nagai, Y., Okumura, K. & Tada, T. A glycolipid on the surface of mouse natural killer cells. *Eur. J. Immunol.* **10**, 175–180 (1980).
7. Kasai, M. et al. In vivo effect of anti-asialo GM1 antibody on natural killer activity. *Nature* **291**, 334–335 (1981).
8. Young, W. W. Jr., Hakomori, S. I., Durdik, J. M. & Henney, C. S. Identification of ganglio-N-tetraosylceramide as a new cell surface marker for murine natural killer (NK) cells. *J. Immunol.* **124**, 199–201 (1980).
9. Zheng, M., Sun, R., Wei, H. & Tian, Z. N. K. Cells help induce anti-hepatitis B virus CD8+ T cell immunity in mice. *J. Immunol.* **196**, 4122–4131 (2016).
10. Mackay, L. K. et al. Long-lived epithelial immunity by tissue-resident memory T (TRM) cells in the absence of persisting local antigen presentation. *Proc. Natl Acad. Sci. USA* **109**, 7037–7042 (2012).
11. Fernandez-Ruiz, D. et al. Liver-resident memory CD8(+) T cells form a front-line defense against malaria liver-stage infection. *Immunity* **45**, 889–902 (2016).
12. Bergsbaken, T. & Bevan, M. J. Proinflammatory microenvironments within the intestine regulate the differentiation of tissue-resident CD8(+) T cells responding to infection. *Nat. Immunol.* **16**, 406–414 (2015).
13. Sheridan, B. S. & Lefrançois, L. Regional and mucosal memory T cells. *Nat. Immunol.* **12**, 485–491 (2011).
14. McNamara, H. A. et al. Up-regulation of LFA-1 allows liver-resident memory T cells to patrol and remain in the hepatic sinusoids. *Sci. Immunol.* **2**, eaaj1996 (2017).
15. Steinert, E. M. et al. Quantifying memory CD8 T cells reveals regionalization of immunosurveillance. *Cell* **161**, 737–749 (2015).
16. Budd, R. C., Cerottini, J. C. & MacDonald, H. R. Phenotypic identification of memory cytolytic T lymphocytes in a subset of Lyt-2+ cells. *J. Immunol.* **138**, 1009–1013 (1987).
17. Richter, M. V. & Topham, D. J. The  $\alpha 1\beta 1$  integrin and TNF receptor II protect airway CD8+ effector T cells from apoptosis during influenza infection. *J. Immunol.* **179**, 5054–5063 (2007).
18. Mackay, L. K. et al. Cutting edge: CD69 interference with sphingosine-1-phosphate receptor function regulates peripheral T cell retention. *J. Immunol.* **194**, 2059–2063 (2015).
19. Stark, R. et al. TRM maintenance is regulated by tissue damage via P2RX7. *Sci. Immunol.* **3**, eaau1022 (2018).
20. Rissiek, B. et al. In vivo blockade of murine ARTC2.2 during cell preparation preserves the vitality and function of liver tissue-resident memory T cells. *Front Immunol.* **9**, 1580 (2018).
21. Kamizono, S. et al. Nfil3/E4bp4 is required for the development and maturation of NK cells in vivo. *J. Exp. Med.* **206**, 2977–2986 (2009).
22. Seillet, C. et al. Nfil3 is required for the development of all innate lymphoid cell subsets. *J. Exp. Med.* **211**, 1733–1740 (2014).
23. Thimme, R. et al. CD8(+) T cells mediate viral clearance and disease pathogenesis during acute hepatitis B virus infection. *J. Virol.* **77**, 68–76 (2003).
24. Tzeng, H. T. et al. PD-1 blockade reverses immune dysfunction and hepatitis B viral persistence in a mouse animal model. *PLoS ONE* **7**, e39179 (2012).
25. Mackay, L. K. et al. Hobit and Blimp1 instruct a universal transcriptional program of tissue residency in lymphocytes. *Science* **352**, 459–463 (2016).
26. Keating, R. et al. Virus-specific CD8+ T cells in the liver: armed and ready to kill. *J. Immunol.* **178**, 2737–2745 (2007).
27. Beura, L. K. et al. T cells in nonlymphoid tissues give rise to lymph-node-resident memory T cells. *Immunity* **48**, 327–338 e325 (2018).
28. Victorino, F. et al. Tissue-Resident NK Cells Mediate Ischemic Kidney Injury and Are Not Depleted by Anti-Asialo-GM1 Antibody. *J. Immunol.* **195**, 4973–4985 (2015).
29. Nishikado, H., Mukai, K., Kawano, Y., Minegishi, Y. & Karasuyama, H. NK cell-depleting anti-asialo GM1 antibody exhibits a lethal off-target effect on basophils in vivo. *J. Immunol.* **186**, 5766–5771 (2011).
30. Kosaka, A. et al. AsialoGM1+CD8+ central memory-type T cells in unimmunized mice as novel immunomodulator of IFN- $\gamma$ -dependent type 1 immunity. *Int. Immunol.* **19**, 249–256 (2007).
31. Slifka, M. K., Pagarigan, R. R. & Whitton, J. L. NK markers are expressed on a high percentage of virus-specific CD8+ and CD4+ T cells. *J. Immunol.* **164**, 2009–2015 (2000).
32. Trambley, J. et al. Asialo GM1(+) CD8(+) T cells play a critical role in costimulation blockade-resistant allograft rejection. *J. Clin. Invest.* **104**, 1715–1722 (1999).
33. Pallett, L. J. et al. IL-2(high) tissue-resident T cells in the human liver: sentinels for hepatotropic infection. *J. Exp. Med.* **214**, 1567–1580 (2017).
34. Tse, S. W., Radtke, A. J., Espinosa, D. A., Cockburn, I. A. & Zavala, F. The chemokine receptor CXCR6 is required for the maintenance of liver memory CD8(+) T cells specific for infectious pathogens. *J. Infect. Dis.* **210**, 1508–1516 (2014).
35. Mackay, L. K. et al. The developmental pathway for CD103(+)CD8+ tissue-resident memory T cells of skin. *Nat. Immunol.* **14**, 1294–1301 (2013).